



Published in final edited form as:

Aging Cell. 2009 September ; 8(5): 573–583. doi:10.1111/j.1474-9726.2009.00508.x.

Effects of Myostatin Deletion in Aging Mice

Michael R. Morissette^{1,*}, Janelle C. Stricker^{1,*}, Michael A. Rosenberg¹, Cattleya Buranasombati¹, Emily B. Levitan¹, Murray A. Mittleman¹, and Anthony Rosenzweig¹

¹Cardiovascular Institute, Beth Israel Deaconess Medical Center and Harvard Medical School, Boston, MA.

Abstract

Inhibitors of myostatin, a negative regulator of skeletal muscle mass, are being developed to mitigate aging-related muscle loss. Knockout mouse studies suggest myostatin also affects adiposity, glucose handling, and cardiac growth. However, the cardiac consequences of inhibiting myostatin remain unclear. Myostatin inhibition can potentiate cardiac growth in specific settings (Morissette *et al.* 2006), a concern since cardiac hypertrophy is associated with adverse clinical outcomes. Therefore we examined the systemic and cardiac effects of myostatin deletion in aged mice (27–30 months old). Heart mass increased comparably in both wildtype (WT) and knockout (KO) mice. Aged KO mice maintained twice as much quadriceps mass as aged WT, however both groups lost the same percentage (36%) of adult muscle mass. Dual-energy x-ray absorptiometry (DEXA) revealed increased bone density, mineral content, and area in aged KO versus aged WT mice. Serum insulin and glucose levels were lower in KO mice. Echocardiography showed preserved cardiac function with better fractional shortening (58.1 vs 49.4%, $p=0.002$) and smaller LV diastolic diameters (3.41 vs 2.71, $p=0.012$) in KO versus WT mice. Phospholamban phosphorylation was increased 3.3-fold in KO hearts ($p<0.05$), without changes in total phospholamban, SERCA2a, or calsequestrin. Aged KO hearts showed less fibrosis by Masson's Trichrome staining. Thus myostatin deletion does not affect aging-related increases in cardiac mass and appears beneficial for bone density, insulin sensitivity, and heart function in senescent mice. These results suggest that clinical interventions designed to inhibit skeletal muscle mass loss with aging could have beneficial effects on other organ systems as well.

Keywords

myostatin; aging; heart; muscle; sarcopenia; osteoporosis

Introduction

Aging is associated with physiological decline in multiple organ systems. Loss of skeletal muscle mass, cardiac hypertrophy, decreased heart function, osteoporosis, and decreased insulin sensitivity, are all associated with aging. Calorie restriction (CR) is recognized as an anti-aging intervention that not only increases life span, but also ameliorates many aging-

Address correspondence to: Anthony Rosenzweig, M.D. Cardiovascular Institute Beth Israel Deaconess Medical Center 3 Blackfan Circle CLS 9 Boston, MA 02215 Phone: 617-735-4200 Fax: 617-735-4202 arosenzw@bidmc.harvard.edu.

*Current address: Division of Exercise Physiology, Center for Cardiovascular and Respiratory Sciences, West Virginia University School of Medicine, Morgantown, WV

MRM: mmorissette@hsc.wvu.edu

JCS: jstricker@hsc.wvu.edu

MAR: marosenb@bidmc.harvard.edu

CB: cattleyab@gmail.com

EBL: elevitan@bidmc.harvard.edu

MAM: mmittlem@bidmc.harvard.edu

related organ specific pathologies (Weindruch 1988). Recently there has been much interest in identifying small molecule CR-mimetics for use in the prevention or delay of aging-related diseases. Of the many metabolic and hormonal changes caused by CR improved insulin sensitivity, decreased glucose levels, and decreased body fat observed in CR mice have been hypothesized to play important roles (Sinclair 2005). In fact a putative CR-mimetic, resveratrol, has been shown to improve metabolic parameters in obese mice (Baur et al. 2006), and aging mice as well (Barger et al. 2008). Interestingly increased muscle mass is also associated with improved glucose and insulin handling and decreased fat mass (Sutrage et al. 1990; Musaro et al. 1999; McPherron & Lee 2002; Lai et al. 2004; Izumiya et al. 2008). It is not known if increased muscle mass has beneficial effects on metabolism and organ function in the aged setting.

Myostatin is a well-known negative regulator of skeletal muscle mass in many species (Grobet et al. 1997; McPherron et al. 1997; McPherron & Lee 1997; Szabo et al. 1998; Clop et al. 2006; Mosher et al. 2007; Shelton & Engvall 2007), including humans (Schuelke et al. 2004). Recently there has been much interest in developing therapeutic inhibitors of myostatin for use in muscle-wasting disorders such as muscular dystrophy, cachexia, or aging-related sarcopenia (Tsuchida 2008). Interestingly one study showed that serum MSTN levels increased with age and that muscle mass was inversely correlated with MSTN serum levels, suggesting an association between MSTN and age-associated sarcopenia (Yarasheski et al. 2002).

Insulin resistance is increased with aging and fat mass. Deletion of myostatin in mouse models of type II diabetes improves glucose metabolism and decreases fat accumulation (McPherron & Lee 2002). Although the loss of myostatin in mice results in increased skeletal muscle mass and decreased adiposity, which could potentially explain the improvements seen in the diabetic models, the exact mechanism has not been defined. Interestingly it is not known if the lean phenotype in the KO mice persists in senescent mice.

Heart size, or more specifically left ventricular hypertrophy (LVH), and heart failure increase with age (Lakatta & Levy 2003). LVH is associated with an increased risk for cardiovascular disease and mortality (Levy et al. 1990). This increase in left ventricular size is characterized by structural remodeling which includes increased cardiomyocyte size with altered calcium handling properties, decreased cardiomyocyte number, and increased collagen deposition (fibrotic replacement of lost cardiomyocytes) (Lakatta & Levy 2003). Studies that have focused on contractile dysfunction in the aging heart have identified decreased sarco(endo)plasmic reticulum calcium ATPase 2a (SERCA2a) function as a possible mediator. SERCA2a function is responsible for transporting calcium from the cytosol into the sarcoplasmic reticulum (SR), and its function is critical for maintaining contractile function. SERCA2a function is negatively regulated by phospholamban, which is inhibited by phosphorylation, which then increases SERCA2a activity. Aging-associated decreases in contractile function have been associated with a decreased SERCA2a-to-PLB ratio (Lim et al. 1999) and total SERCA2a protein levels (Schmidt et al. 2000; Li et al. 2007). Interestingly, restoration of contractile function in aged hearts was achieved by increasing SERCA2a protein expression back to the level seen in adult hearts (Schmidt et al. 2000).

We (Morissette et al. 2006) and others (Reisz-Porszasz et al. 2003) have found that myostatin can affect cardiac muscle growth as well, which underscores the importance of understanding how myostatin affects the size and function of the heart in settings where inhibitors, such as aging, might be used. In order to understand the effects of myostatin in aging, we studied a cohort of senescent myostatin knock-out mice (KO), and their wild-type littermates (WT), at 27-30 months old. We measured heart and skeletal muscle mass and

compared them to adult (4-5 months old) values. DEXA scanning was used to determine the effect of myostatin deletion on bone composition in senescent mice. Serum glucose and insulin, along with possible endocrine mediators of insulin sensitivity, were measured. To evaluate in vivo cardiac function we performed echocardiography on both cohorts of aged mice. To determine possible mechanisms related to the changes in heart function observed we examined biochemical changes in key cardiac calcium handling proteins, and measured cardiac fibrosis.

Results

During normal aging, increases in cardiac mass (Lakatta & Levy 2003) and decreases in skeletal muscle mass (Thompson 2008) have been observed. To determine if the loss of myostatin modulates these processes we compared adult and senescent heart and quadriceps mass in WT and KO mice.

Both WT and KO heart mass increased with age compared to adult heart mass (WT $p<0.0001$; KO $p<0.001$, Figure 1A). The extent of age-related growth between WT and KO mice was similar (25.0% and 30.6% respectively, $p=ns$), and there was no difference between WT and KO heart mass in either the adult or senescent group. From these data we conclude that the loss of myostatin did not result in more exuberant cardiac growth with aging.

Consistent with previous reports (McPherron *et al.* 1997), adult (4-5 month old) KO mice exhibited 2.2-fold greater quadriceps muscle mass compared to WT (167.1 ± 2.4 vs 372.0 ± 13.0 mg, $p<0.001$, Figure 1B). Senescent WT and KO mice each had less muscle mass than adults of the same genotype, however the senescent KO mice maintained more muscle mass compared to WT (106.3 ± 6.3 vs 234.9 ± 12.4 mg, $p<0.001$, Figure 1B). Interestingly, the percent muscle mass loss with aging was remarkably similar in both WT and KO groups (36.4% vs 36.8%). Consistent with previous reports, total body mass was significantly higher in the adult KO versus WT (34.2 ± 1.1 vs 28.6 ± 1.0 g, $p<0.01$, Figure 1C) mainly due to the increase in skeletal muscle mass (McPherron *et al.* 1997). Aged WT mice showed an increase in body mass compared adult mice ($p<0.01$, Figure 1C), likely due to increases in fat mass, while there was no significant increase in aged KO compared to adult KO total body mass.

Adult myostatin KO mice have been reported to have decreased body fat (McPherron & Lee 2002). To assess the effect of aging on body mass composition, we performed dual-energy x-ray absorptiometry (DEXA) scans on adult and senescent (27-30 months old) WT and KO mice. Interestingly body fat percentage was 2-fold lower in the KO compared to WT (Figure 2B, $p<0.05$). There was a non-significant trend towards increased lean tissue and decreased total fat in senescent KO mice (Figure 2B). Total body weight between senescent WT and KO mice was not different by direct measurement (Figure 1C) or DEXA (Figure 2B).

Bone mineral density (BMD, Figure 2C, 0.051 ± 0.0005 vs 0.055 ± 0.0012 g/cm², $p<0.01$), bone mineral content (BMC, Figure 2D, 0.45 ± 0.02 vs 0.54 ± 0.016 g, $p<0.01$) and bone area (Figure 2B, 8.81 ± 0.034 vs 9.77 ± 0.19 cm², $p<0.05$) in KO mice were increased compared to WT controls suggesting that the loss of myostatin may inhibit aging-related bone loss.

To determine if the KO mice are resistant to age-related loss of insulin sensitivity, we measured serum insulin and blood glucose in senescent WT and KO mice. We found that aged KO mice had lower levels of both random insulin (Figure 3A; 155.5 ± 22.2 vs 77.9 ± 7.9 pmol/L, $p=0.008$) and glucose (Figure 3B; 8.9 ± 0.7 vs 6.7 ± 0.5 mmol/L, $p<0.04$), suggesting improved insulin sensitivity. Based on these data we used homeostatic model assessment

(HOMA)(Levy *et al.* 1998) to estimate insulin resistance, and found scores consistent with better insulin sensitivity in KO mice (3.4 ± 0.4 vs 1.5 ± 0.2 , $p<0.002$, $n= 14$ WT, 10 KO).

Circulating IGF-I levels have been shown to decrease with age in both rodents and humans (Harman 2004). Skeletal muscle-specific IGF-I overexpression results in increased muscle mass (Musaro *et al.* 1999), and cardiac-restricted transgenic overexpression of IGF-I prevents age-associated decrease in heart function and failure (Torella *et al.* 2004). For these reasons an increase in IGF-I levels would be consistent with the skeletal muscle and cardiac phenotypes in the senescent KO mice. However, IGF-I levels were not different between senescent WT or KO mice (Figure 3A, 169.4 ± 22.7 vs 159.8 ± 21.8 ng/ml, $p=ns$), suggesting circulating IGF-I is not responsible for the improved cardiac function or increased muscle mass in aged KO mice.

Since young KO mice have been reported to have less fat and smaller adipocytes (McPherron & Lee 2002), which may be associated with favorable metabolic effects (Feldman *et al.* 2006), we examined levels of two fat-secreted adipokines, adiponectin and retinol binding protein-4 (RBP4), that could contribute to enhanced insulin sensitivity. Adiponectin secretion is inversely proportional to fat mass, and low levels of adiponectin are associated with insulin resistance (Yamauchi *et al.* 2001). RBP4 is an adipokine that is increased in humans with obesity and type II diabetes, and has been shown to contribute to insulin resistance in mice (Yang *et al.* 2005). Serum levels of RBP4 were lower in adult MSTN KO versus WT mice. However, we found no difference between levels of either adiponectin (Figure 3B) or RBP4 (Figure 3C) in serum from aged WT and KO mice, although there was a nonsignificant trend toward decreased adiponectin in KO mice. Since high levels of adiponectin are associated with enhanced insulin sensitivity, we would have expected to see an increase in adiponectin in the aged MSTN KO mice. Since we did not see increased levels of adiponectin in the aged MSTN KO mice, we conclude that adiponectin is not responsible for the improved glucose and insulin parameters. In addition, free fatty acids (FFA) did not differ between the two groups of mice (Figure 3B, WT 1.55 ± 0.23 vs KO 1.95 ± 0.85 , $p=ns$).

To determine if myostatin deletion affects heart function in senescent mice, we performed echocardiography in unanesthetized male WT and KO mice, aged 27-30 months old. Previously we have published that cardiac function (mean fractional shortening, a measure of systolic heart function, ~64%) and chamber dimensions measured by echocardiography were not different in young adult KO and WT mice (Morissette *et al.* 2006). In contrast, senescent KO mice show better preserved fractional shortening compared to similarly aged WT mice (58.1 vs 49.4% , $p=0.002$) (Figure 4B). In addition, the KO mice showed less chamber dilation, which increases in heart failure, as evidenced by smaller LV diastolic (2.71 vs 3.41 mm, $p=0.012$) and LV systolic diameters (1.15 vs 1.72 mm, $p=0.002$) in KO mice (Figure 4C). Although there was a trend towards increased wall thickness in the KO hearts, this difference was not significant compared to WT hearts (Figure 4D). These data suggest that the deletion of myostatin protects the heart from age-associated loss of contractile function.

In order to determine the molecular mechanisms responsible for the differences in heart function between aged MSTN KO and WT mice, we examined the levels of the key proteins controlling cardiomyocyte function through regulation of calcium handling. SERCA2a is responsible for transporting calcium from the cytosol into the sarcoplasmic reticulum (SR), and its function is critical for maintaining contractile function. Phospholamban binds to SERCA2a and negatively regulates its activity without changing its expression. Phosphorylation of phospholamban inhibits its binding to SERCA2a and thereby increases SERCA2a activity (Bers 2008). Although decreased SERCA2a protein levels have been

reported in aged mouse hearts (Li *et al.* 2007), we did not see a difference in SERCA2a protein expression between WT and KO mice (Figure 5A,B). Similarly, total phospholamban levels were not different in KO and WT hearts. However, we did observe a substantial (3.3-fold) increase in the ratio of phosphorylated phospholamban (PLB) to total PLB in the KO hearts ($p < 0.05$, Figure 5B) compared to WT, which would reduce PLB-mediated inhibition of SERCA2a. Calsequestrin levels, which were not different between WT and KO, were used to normalize protein levels and serve as a control for SR protein isolation (Figure 5A,B). Thus the observed higher level of PLB phosphorylation may contribute to the better contractile function observed in the KO hearts.

Cardiac fibrosis has been shown to increase with age and is thought to contribute to a decrease in cardiac (diastolic) function (Lakatta & Levy 2003; Sussman & Anversa 2004; Alcendor *et al.* 2007). Since myostatin has been demonstrated to have a pro-fibrotic role in skeletal muscle (McCroskery *et al.* 2005; Parsons *et al.* 2006; Li *et al.* 2008), we examined fibrosis in adult and senescent hearts from WT and KO mice. Fibrosis was almost undetectable in adult hearts as expected. Quantitation of fibrosis on Masson's Trichrome stained heart sections revealed a 2.4-fold increase in fibrosis in WT compared to KO hearts (Figure 6, $p = 0.02$). This decrease in fibrosis, along with the increased phosphorylation of phospholamban, may explain the preservation of cardiac function seen in the KO mice.

Despite the beneficial effects observed in cardiac function and insulin sensitivity, we did not observe an increase in overall survival in the MSTN KO mice (see Supplemental Figure S1). However, since the initial aims of this study did not include longevity analysis, the current study was statistically underpowered to detect even a 2-3 month difference in survival. Thus additional studies in larger cohorts would be required to definitively address this issue.

Discussion

The goal of this study was to gain insight into the effects of myostatin inhibition, using a chronic genetic deletion mouse model, on multiple organ systems in the setting of aging.

Since myostatin is a negative regulator of muscle mass it has been implicated in aging-related sarcopenia (Siriatt *et al.* 2006). Here we show that WT and KO mice lost muscle mass to the same extent with aging, suggesting that while the KO mice start with greater muscle mass, deletion of myostatin does not inhibit the biological processes underlying aging-related muscle mass loss. These data would argue against a specific role for myostatin as a mediator of sarcopenia. Previously, reduced muscle fiber atrophy (type IIb/X) in two year-old KO mice compared to similarly aged WT mice was reported, however no measurements of overall skeletal muscle mass was reported so it was not possible to determine if they saw similar aging-related muscle mass loss as we report here (Siriatt *et al.* 2006). Whether myostatin inhibition in adult animals or people would nevertheless have benefits in sarcopenia through an overall increase in muscle mass obviously cannot be addressed by our data in germline KO mice.

The loss of bone integrity or osteoporosis in aged individuals is an important clinical problem. We observed increased bone mineral density, content, and area in aged MSTN KO mice compared to aged WT. Although we cannot rule out the possibility that increased bone density is due to increased stress on the bone at the ligament insertion sites secondary to increased muscle mass (Hamrick *et al.* 2002), it is also possible that the loss of myostatin itself or the favorable metabolic changes seen in the MSTN KO mice may directly affect bone remodeling (Kellum *et al.* 2009). Thus inhibition of myostatin may be beneficial in the setting of aging-related osteoporosis.

Lower serum glucose and insulin levels in aged KO versus WT mice suggest that the inhibition of myostatin may preserve insulin sensitivity with aging. We did not find any differences in adiponectin or RBP4 in senescent mice that would explain preservation of insulin sensitivity in the KO mice, however adult MSTN KO mice had decreased serum levels of RBP4. Although the difference in RBP4 is not maintained until the age at which we see decreased insulin and glucose in the MSTN KO mice, one could speculate that improved glucose handling at a young age secondary to low RBP4 levels may provide a metabolic “memory” or “legacy” effect, similar to intensive glycemic control in type II diabetics that show benefits after long-term follow-up despite the cessation of intensive therapy (Holman *et al.* 2008). Although the loss of myostatin in mouse models of type-II diabetes improves glucose handling, no differences in baseline serum glucose and insulin levels were reported in adult KO compared to WT mice (McPherron & Lee 2002; Guo *et al.* 2009). It remains unclear whether the increased muscle mass seen in the aged KO mice completely explains the preservation of insulin sensitivity or if myostatin has additional direct effects on critical signaling pathways involved in glucose homeostasis. For instance increased glucose utilization may be sufficient to explain this phenotype since the increase in muscle mass seen with MSTN KO mice is due to an increase in fast glycolytic muscle fibers (McPherron *et al.* 1997). Furthermore other genetically-modified mice that exhibit increased muscle mass have less fat mass similar to the MSTN KO mice (Sutrave *et al.* 1990; Musaro *et al.* 1999; Lai *et al.* 2004; Izumiya *et al.* 2008), which may affect adipokines and insulin sensitivity secondary to increased muscle mass. However direct effects of loss of myostatin on skeletal muscle may also play a role (Guo *et al.* 2009). For instance we have previously demonstrated that myostatin can inhibit Akt, a critical mediator of insulin mediated glucose uptake. Thus increased Akt activation in insulin sensitive tissues could contribute to increased glucose uptake and preserved insulin sensitivity.

Cardiac hypertrophy is often characterized as pathological, which is associated with adverse outcomes including heart failure and arrhythmia, or physiological, which is not. In addition, it seems likely that more subtle distinctions among cardiac growth in response to specific stimuli exist. Previously, we have found that myostatin regulates cardiomyocyte growth in a stimulus-specific manner, and it was unclear whether this could exacerbate pathological hypertrophy in some settings (Morissette *et al.* 2006). Here we examined the effects of myostatin deletion in senescent mice and found that KO mice exhibited a similar increase in cardiac mass with aging as WT littermates, suggesting myostatin is not a negative regulator of the hypertrophic growth seen with aging. Its role in other specific circumstance such as the response to hemodynamic stress will need to be addressed separately. Surprisingly, we found that the loss of myostatin resulted in preserved cardiac function in senescent mice compared to WT controls. A recent study demonstrating mitochondrial depletion and a decrease in force generation in MSTN KO skeletal muscle (Amthor *et al.* 2007) suggests cardiac function could be impaired in MSTN KO mice if the heart were similarly affected. The observed *increase* in function in the MSTN KO mice suggests that either cardiac muscle force and mitochondria are not decreased or additional stress is required to reveal a phenotype. These data suggest that systemic inhibition of myostatin intended to ameliorate aging-related sarcopenia would not be expected to cause hypertrophy and could actually benefit heart function.

Another group has also looked at aged cohorts of WT and KO mice (Cohn *et al.* 2007), and did not find any differences in cardiac function or fibrosis between the groups. One potential explanation for the difference is that they studied a younger cohort (24 month-old) of mice, in which the decrease in function and increase in fibrosis in the WT animals may not yet be manifest. Technical differences in measuring function and fibrosis may also contribute to the discrepant results. For example, we measured cardiac function in conscious mice with physiologically relevant heart rates, while their measurements were obtained from deeply

anesthetized mice. The use of anesthetic is known to decrease fractional shortening and heart rate (Rottman *et al.* 2007), while introducing temporal variability into these measurements (Rottman *et al.* 2003), potentially making it harder to detect significant differences.

It is unclear if the effects on cardiac function are directly related to the loss of myostatin itself or secondary to the metabolic changes observed in the KO mice. Recent work has demonstrated that activation of Akt in skeletal muscle is sufficient to mediate multiple beneficial metabolic effects (Izumiya *et al.* 2008), and similar cross-talk could extend to the heart as well. In fact, beneficial effects on metabolism in aged mice subjected to CR or resveratrol were also associated with improved cardiac function (Barger *et al.* 2008). Given our previous observation that myostatin has direct effects in cardiomyocytes (Morissette *et al.* 2006), it seems likely that both direct and indirect effects are contributing. The increase in phosphorylation of PLB that we report here in the KO hearts not only provides a possible mechanism for the preserved contractile function observed, but also suggests that the loss of myostatin may enhance the response to adrenergic stimulation in these hearts. We have previously shown enhanced p38 phosphorylation in response to *in vivo* α -adrenergic stimulation in myostatin KO hearts (Morissette *et al.* 2006). Increased phosphorylation of PLB secondary to a compensatory increase in adrenergic stimulation has been shown to initially preserve cardiac function in mice with cardiac-specific overexpression of PLB (Dash *et al.* 2001; Dash *et al.* 2003), thus the increased cardiac function seen in the KO mice may be mechanistically linked to enhanced adrenergic signaling due to the loss of myostatin.

In conclusion, we report that the chronic loss of myostatin in senescent mice results in improved cardiac function, decreased cardiac fibrosis, preserved bone density parameters, and better glucose and insulin profiles compared to WT controls. These data suggest that the potential use of myostatin inhibitors to treat sarcopenia in aged individuals could also have beneficial effects on the heart, bone, and endocrine function as well. However, caution is warranted in directly extrapolating results from a mouse model of chronic genetic deletion model to administration of an inhibitor to an adult or human.

Experimental Procedures

Mice

Myostatin knock-out (KO) mice (McPherron *et al.* 1997) were kindly provided by Dr. Se Jin Lee (Johns Hopkins University). Mice were backcrossed to C57BL/6 for ≥ 6 generations and littermate controls were used in all data presented. Senescent mice used for this study were between 27-30 months old, slightly above the reported median lifespan (age at which 50% are dead) for C57BL/6 mice (Anver 2004). Adult mice were between 16-20 weeks old. Bone density and body composition were measured in isoflurane anesthetized mice by dual-energy x-ray absorptiometry (DEXA, Lunar PIXImus2 mouse densitometer). All studies were approved by the Institutional Animal Care and Use Committee at Beth Israel Deaconess Medical Center and were conducted in accordance with the principles and procedures outlined in the National Institutes of Health Guide for Care and Use of Laboratory Animals.

Tissue preparation and Immunoblotting

Protein from 27-30 month old mouse hearts was obtained after the atria were removed. Briefly, muscle tissue from mice were harvested, rinsed in cold PBS, snap frozen in liquid nitrogen, and homogenized in lysis buffer (Cell Signalling, Beverly, MA) plus 5 mM Phenylmethylsulphonyl fluoride (PMSF), followed by centrifugation at 20,000 \times g for 10 minutes at 4 $^{\circ}$ C. Protein concentration was determined by Bradford Assay (Bio-Rad,

Hercules, CA) and equal amounts of protein (~100 µg) in loading buffer were warmed to 37° C (to prevent dissociation of phospholamban pentamer) and loaded in each lane of a 4-15% pre-cast tris-glycine/sodium dodecyl sulfate-polyacrylamide gel (Bio-Rad). Proteins were separated by electrophoresis, transferred (semi-dry, Bio-Rad) to nitrocellulose membranes, and incubated overnight at 4° C with indicated antibody diluted (1:1000) in 5% non-fat powdered milk/tris-buffered saline/0.1% tween (TBST). Blots were incubated with rat anti-RBP4 (DakoCytomation, Denmark) (Yang *et al.* 2005), anti-phospholamban, anti-phospho-phospholamban (S16) (Upstate, Lake Placid, NY), anti-SERCA2a (Affinity Bioreagents, Golden, CO), anti-calsquestrin (Abcam, Cambridge, MA), anti-GAPDH, (Cell Signaling, Beverly, MA), overnight at 4°C and subsequently incubated with HRP-conjugated secondary antibody (1:5000; DakoCytomation), and detected by chemiluminescence (Cell Signaling).

Measurement of metabolic parameters

All metabolic parameters were measured from blood collected between 8-10 am. All measurements were made from serum of random fed mice unless otherwise noted. Glucose was measured using a blood sample from the tail vein using a OneTouch glucometer (LifeScan, CA). Insulin (Crystal Chem, INC, IL), adiponectin (Millipore, MO), and IGF-I (Diagnostic Systems Laboratories, TX) levels were determined by commercial enzyme-linked immunosorbent assay (ELISA) kits according to the manufacturer's protocol. Serum free-fatty acids were measured in fasted animals using the NEFA-C kit (Wako, VA). Serum RBP4 was measured by running a western blot with 1µl of serum (diluted 20X in lysis buffer) as previously described (Yang *et al.* 2005), using a rat anti-RBP4 antibody.

Echocardiography

Echocardiography was performed on unanesthetized mice using a 13L high-frequency linear (10 MHz) transducer (VingMed 5, GE Medical Services) with depth set at 1cm and 236 frames/second for 2-dimensional (2-D) images. M-mode images used for measurements were taken at the papillary muscle level.

Fibrosis Measurements

Mid-ventricular short axis heart sections from male WT and KO mice were fixed in formalin and six 5 m sections stained with Masson's trichrome to visualize fibrotic tissue. In order to objectively quantify the amount of tissue fibrosis, we developed a pre-specified, genotype-blinded image selection method. Images were selected for analysis such that the image selected from each section contained the largest amount of fibrosis for that particular section. Preliminary studies determined that 20x magnification was optimal for distinguishing the amount of interstitial fibrosis present in the heart sections. Percent fibrosis was determined using CellProfiler Image Analysis software (Lamprecht *et al.* 2007) to quantitate blue (fibrotic) versus non-blue (non-fibrotic) pixels. The results are presented as percent fibrosis/image area (not whole heart). Given the clustered nature of the data, statistical analysis was performed using mixed-effects linear regression, with clustering analyzed at the level of the mouse.

Muscle Mass Determination

The mass of hearts from which vessels but not atria were removed, was determined after quickly rinsing in cold phosphate buffered saline (PBS), and blotting dry on a paper towel. Skeletal muscle mass was determined by dissecting the same muscle from both the left and right sides of the mouse, removing the fascia, rinsing in cold PBS, and blotting dry. The mass of both sides were averaged to yield reported muscle mass.

Statistics

Data are represented as mean±SEM and compared by 2-tailed Student's t-test, except for fibrosis quantitation (see Fibrosis Measurements above). The null hypothesis was rejected for $p < 0.05$.

Supplementary Material

Refer to Web version on PubMed Central for supplementary material.

Acknowledgments

We thank the BIDMC Metabolic Physiology Core of NIDDK P30 for the facilitating the DEXA scan studies and consultation on measurement of serum components, and Dr. Serafima Zaltsman for expertly managing the mouse colony. This research was supported by a Leduq Foundation Network of Research Excellence (SAC, AR) and grants from the NIH: Award Number K01AG026337 from the National Institute on Aging (MRM), and R01HL61557 from the NHLBI (AR). The content is solely the responsibility of the authors and does not necessarily represent the official views of the National Institute on Aging or the National Institutes of Health. AR is a principal faculty member of the Harvard Stem Cell Institute.

References

- Alcendor RR, Gao S, Zhai P, Zablocki D, Holle E, Yu X, Tian B, Wagner T, Vatner SF, Sadoshima J. Sirt1 regulates aging and resistance to oxidative stress in the heart. *Circ Res*. 2007; 100:1512–1521. [PubMed: 17446436]
- Amthor H, Macharia R, Navarrete R, Schuelke M, Brown SC, Otto A, Voit T, Muntoni F, Vrbova G, Partridge T, Zammit P, Bunker L, Patel K. Lack of myostatin results in excessive muscle growth but impaired force generation. *Proc Natl Acad Sci U S A*. 2007; 104:1835–1840. [PubMed: 17267614]
- Hedrich, H., editor. In *The Laboratory Mouse*. Elsevier; 2004. Gerontology.
- Barger JL, Kayo T, Vann JM, Arias EB, Wang J, Hacker TA, Wang Y, Raederstorff D, Morrow JD, Leeuwenburgh C, Allison DB, Saupe KW, Cartee GD, Weindruch R, Prolla TA. A low dose of dietary resveratrol partially mimics caloric restriction and retards aging parameters in mice. *PLoS ONE*. 2008; 3:e2264. [PubMed: 18523577]
- Baur JA, Pearson KJ, Price NL, Jamieson HA, Lerin C, Kalra A, Prabhu VV, Allard JS, Lopez-Lluch G, Lewis K, Pistell PJ, Poosala S, Becker KG, Boss O, Gwinn D, Wang M, Ramaswamy S, Fishbein KW, Spencer RG, Lakatta EG, Le Couteur D, Shaw RJ, Navas P, Puigserver P, Ingram DK, de Cabo R, Sinclair DA. Resveratrol improves health and survival of mice on a high-calorie diet. *Nature*. 2006; 444:337–342. [PubMed: 17086191]
- Bers DM. Calcium cycling and signaling in cardiac myocytes. *Annu Rev Physiol*. 2008; 70:23–49. [PubMed: 17988210]
- Clop A, Marcq F, Takeda H, Pirottin D, Tordoir X, Bibe B, Bouix J, Caiment F, Elsen JM, Eychenne F, Larzul C, Laville E, Meish F, Milenkovic D, Tobin J, Charlier C, Georges M. A mutation creating a potential illegitimate microRNA target site in the myostatin gene affects muscularity in sheep. *Nature Genetics*. 2006; 38:813–818. [PubMed: 16751773]
- Cohn RD, Liang HY, Shetty R, Abraham T, Wagner KR. Myostatin does not regulate cardiac hypertrophy or fibrosis. *Neuromuscul Disord*. 2007; 17:290–296. [PubMed: 17336525]
- Dash R, Kadambi V, Schmidt AG, Tepe NM, Biniakiewicz D, Gerst MJ, Canning AM, Abraham WT, Hoit BD, Liggett SB, Lorenz JN, Dorn GW 2nd, Kranias EG. Interactions between phospholamban and beta-adrenergic drive may lead to cardiomyopathy and early mortality. *Circulation*. 2001; 103:889–896. [PubMed: 11171800]
- Dash R, Schmidt AG, Pathak A, Gerst MJ, Biniakiewicz D, Kadambi VJ, Hoit BD, Abraham WT, Kranias EG. Differential regulation of p38 mitogen-activated protein kinase mediates gender-dependent catecholamine-induced hypertrophy. *Cardiovasc Res*. 2003; 57:704–714. [PubMed: 12618232]

- Feldman BJ, Streeper RS, Farese RV Jr, Yamamoto KR. Myostatin modulates adipogenesis to generate adipocytes with favorable metabolic effects. *Proc Natl Acad Sci U S A*. 2006; 103:15675–15680. [PubMed: 17030820]
- Grobet L, Martin LJ, Poncelet D, Pirottin D, Brouwers B, Riquet J, Schoeberlein A, Dunner S, Menissier F, Massabanda J, Fries R, Hanset R, Georges M. A deletion in the bovine myostatin gene causes the double-muscling phenotype in cattle. *Nature Genetics*. 1997; 17:71–74. [PubMed: 9288100]
- Guo T, Jou W, Chanturiya T, Portas J, Gavrilova O, McPherron AC. Myostatin inhibition in muscle, but not adipose tissue, decreases fat mass and improves insulin sensitivity. *PLoS ONE*. 2009; 4:e4937. [PubMed: 19295913]
- Hamrick MW, McPherron AC, Lovejoy CO. Bone mineral content and density in the humerus of adult myostatin-deficient mice. *Calcif Tissue Int*. 2002; 71:63–68. [PubMed: 12060865]
- Harman SM. What do hormones have to do with aging? What does aging have to do with hormones? *Annals Of The New York Academy Of Sciences*. 2004; 1019:299–308. [PubMed: 15247033]
- Holman RR, Paul SK, Bethel MA, Matthews DR, Neil HA. 10-year follow-up of intensive glucose control in type 2 diabetes. *N Engl J Med*. 2008; 359:1577–1589. [PubMed: 18784090]
- Izumiya Y, Hopkins T, Morris C, Sato K, Zeng L, Viereck J, Hamilton JA, Ouchi N, LeBrasseur NK, Walsh K. Fast/Glycolytic muscle fiber growth reduces fat mass and improves metabolic parameters in obese mice. *Cell Metab*. 2008; 7:159–172. [PubMed: 18249175]
- Kellum E, Starr H, Arounleut P, Immel D, Fulzele S, Wenger K, Hamrick MW. Myostatin (GDF-8) deficiency increases fracture callus size, Sox-5 expression, and callus bone volume. *Bone*. 2009; 44:17–23. [PubMed: 18852073]
- Lai KM, Gonzalez M, Poueymirou WT, Kline WO, Na E, Zlotchenko E, Stitt TN, Economides AN, Yancopoulos GD, Glass DJ. Conditional activation of akt in adult skeletal muscle induces rapid hypertrophy. *Mol Cell Biol*. 2004; 24:9295–9304. [PubMed: 15485899]
- Lakatta EG, Levy D. Arterial and cardiac aging: major shareholders in cardiovascular disease enterprises: Part II: the aging heart in health: links to heart disease. *Circulation*. 2003; 107:346–354. [PubMed: 12538439]
- Lamprecht MR, Sabatini DM, Carpenter AE. CellProfiler: free, versatile software for automated biological image analysis. *Biotechniques*. 2007; 42:71–75. [PubMed: 17269487]
- Levy D, Garrison RJ, Savage DD, Kannel WB, Castelli WP. Prognostic implications of echocardiographically determined left ventricular mass in the Framingham Heart Study. *N Engl J Med*. 1990; 322:1561–1566. [PubMed: 2139921]
- Levy JC, Matthews DR, Hermans MP. Correct homeostasis model assessment (HOMA) evaluation uses the computer program. *Diabetes Care*. 1998; 21:2191–2192. [PubMed: 9839117]
- Li Q, Wu S, Li SY, Lopez FL, Du M, Kajstura J, Anversa P, Ren J. Cardiac-specific overexpression of insulin-like growth factor 1 attenuates aging-associated cardiac diastolic contractile dysfunction and protein damage. *Am J Physiol Heart Circ Physiol*. 2007; 292:H1398–1403. [PubMed: 17085535]
- Li ZB, Kollias HD, Wagner KR. Myostatin directly regulates skeletal muscle fibrosis. *J Biol Chem*. 2008; 283:19371–19378. [PubMed: 18453534]
- Lim CC, Liao R, Varma N, Apstein CS. Impaired lusitropy-frequency in the aging mouse: role of Ca(2+)-handling proteins and effects of isoproterenol. *Am J Physiol*. 1999; 277:H2083–2090. [PubMed: 10564164]
- McCroskery S, Thomas M, Platt L, Hennebry A, Nishimura T, McLeay L, Sharma M, Kambadur R. Improved muscle healing through enhanced regeneration and reduced fibrosis in myostatin-null mice. *Journal Of Cell Science*. 2005; 118:3531–3541. [PubMed: 16079293]
- McPherron AC, Lawler AM, Lee SJ. Regulation of skeletal muscle mass in mice by a new TGF-beta superfamily member. *Nature*. 1997; 387:83–90. [PubMed: 9139826]
- McPherron AC, Lee SJ. Double muscling in cattle due to mutations in the myostatin gene. *Proc Natl Acad Sci U S A*. 1997; 94:12457–12461. [PubMed: 9356471]
- McPherron AC, Lee SJ. Suppression of body fat accumulation in myostatin-deficient mice. *J Clin Invest*. 2002; 109:595–601. [PubMed: 11877467]

- Morissette MR, Cook SA, Foo S, McKoy G, Ashida N, Novikov M, Scherrer-Crosbie M, Li L, Matsui T, Brooks G, Rosenzweig A. Myostatin regulates cardiomyocyte growth through modulation of Akt signaling. *Circ Res.* 2006; 99:15–24. [PubMed: 16763166]
- Mosher DS, Quignon P, Bustamante CD, Sutter NB, Mellersh CS, Parker HG, Ostrander EA. A mutation in the myostatin gene increases muscle mass and enhances racing performance in heterozygote dogs. *PLoS Genet.* 2007; 3:e79. [PubMed: 17530926]
- Musaro A, McCullagh KJ, Naya FJ, Olson EN, Rosenthal N. IGF-1 induces skeletal myocyte hypertrophy through calcineurin in association with GATA-2 and NF-ATc1. *Nature.* 1999; 400:581–585. [PubMed: 10448862]
- Parsons SA, Millay DP, Sargent MA, McNally EM, Molkentin JD. Age-dependent effect of myostatin blockade on disease severity in a murine model of limb-girdle muscular dystrophy. *Am J Pathol.* 2006; 168:1975–1985. [PubMed: 16723712]
- Reisz-Porszasz S, Bhasin S, Artaza JN, Shen R, Sinha-Hikim I, Hogue A, Fielder TJ, Gonzalez-Cadavid NF. Lower skeletal muscle mass in male transgenic mice with muscle-specific overexpression of myostatin. *Am J Physiol Endocrinol Metab.* 2003; 285:E876–888. [PubMed: 12824080]
- Rottman JN, Ni G, Brown M. Echocardiographic evaluation of ventricular function in mice. *Echocardiography.* 2007; 24:83–89. [PubMed: 17214630]
- Rottman JN, Ni G, Khoo M, Wang Z, Zhang W, Anderson ME, Madu EC. Temporal changes in ventricular function assessed echocardiographically in conscious and anesthetized mice. *J Am Soc Echocardiogr.* 2003; 16:1150–1157. [PubMed: 14608286]
- Schmidt U, del Monte F, Miyamoto MI, Matsui T, Gwathmey JK, Rosenzweig A, Hajjar RJ. Restoration of diastolic function in senescent rat hearts through adenoviral gene transfer of sarcoplasmic reticulum Ca(2+)-ATPase. *Circulation.* 2000; 101:790–796. [PubMed: 10683354]
- Schuelke M, Wagner KR, Stolz LE, Hubner C, Riebel T, Komen W, Braun T, Tobin JF, Lee SJ. Myostatin mutation associated with gross muscle hypertrophy in a child. *N Engl J Med.* 2004; 350:2682–2688. [PubMed: 15215484]
- Shelton GD, Engvall E. Gross muscle hypertrophy in whippet dogs is caused by a mutation in the myostatin gene. *Neuromuscul Disord.* 2007; 17:721–722. [PubMed: 17651971]
- Sinclair DA. Toward a unified theory of caloric restriction and longevity regulation. *Mech Ageing Dev.* 2005; 126:987–1002. [PubMed: 15893363]
- Siriatt V, Platt L, Salerno MS, Ling N, Kambadur R, Sharma M. Prolonged absence of myostatin reduces sarcopenia. *J Cell Physiol.* 2006; 209:866–873. [PubMed: 16972257]
- Sussman MA, Anversa P. Myocardial aging and senescence: where have the stem cells gone? *Annu Rev Physiol.* 2004; 66:29–48. [PubMed: 14977395]
- Sutrave P, Kelly AM, Hughes SH. ski can cause selective growth of skeletal muscle in transgenic mice. *Genes Dev.* 1990; 4:1462–1472. [PubMed: 2253874]
- Szabo G, Dallmann G, Muller G, Patthy L, Soller M, Varga L. A deletion in the myostatin gene causes the compact (Cmpt) hypermuscular mutation in mice. *Mamm Genome.* 1998; 9:671–672. [PubMed: 9680391]
- Thompson LV. Age-related muscle dysfunction. *Exp Gerontol.* 2008
- Torella D, Rota M, Nurzynska D, Musso E, Monsen A, Shiraiishi I, Zias E, Walsh K, Rosenzweig A, Sussman MA, Urbanek K, Nadal-Ginard B, Kajstura J, Anversa P, Leri A. Cardiac stem cell and myocyte aging, heart failure, and insulin-like growth factor-1 overexpression. *Circ Res.* 2004; 94:514–524. [PubMed: 14726476]
- Tsuchida K. Targeting myostatin for therapies against muscle-wasting disorders. *Curr Opin Drug Discov Devel.* 2008; 11:487–494.
- Weindruch, R.; Walford, RL. *The Retardation of Aging and Disease by Dietary Restriction.* Springfield, IL: 1988.
- Yamauchi T, Kamon J, Waki H, Terauchi Y, Kubota N, Hara K, Mori Y, Ide T, Murakami K, Tsuboyama-Kasaoka N, Ezaki O, Akanuma Y, Gavrilova O, Vinson C, Reitman ML, Kagechika H, Shudo K, Yoda M, Nakano Y, Tobe K, Nagai R, Kimura S, Tomita M, Froguel P, Kadowaki T. The fat-derived hormone adiponectin reverses insulin resistance associated with both lipoatrophy and obesity. *Nat Med.* 2001; 7:941–946. [PubMed: 11479627]

- Yang Q, Graham TE, Mody N, Preitner F, Peroni OD, Zabolotny JM, Kotani K, Quadro L, Kahn BB. Serum retinol binding protein 4 contributes to insulin resistance in obesity and type 2 diabetes. *Nature*. 2005; 436:356–362. [PubMed: 16034410]
- Yarasheski KE, Bhasin S, Sinha-Hikim I, Pak-Loduca J, Gonzalez-Cadavid NF. Serum myostatin-immunoreactive protein is increased in 60-92 year old women and men with muscle wasting. *J Nutr Health Aging*. 2002; 6:343–348. [PubMed: 12474026]

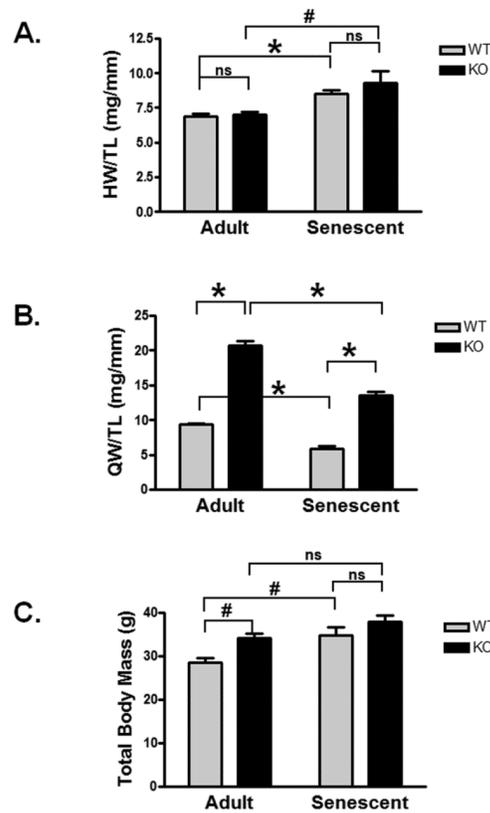


Figure 1. Morphometric changes in senescent mice

A) Heart/tibial length (mg/mm) [adult WT, KO, senescent WT, KO; n=9,10,7,4] B) quadriceps mass/tibial length (g/mm) [adult WT, KO, senescent WT, KO; n=5,7,7,4], and C) total body (g) [adult WT, KO, senescent WT, KO; n=9,10,8,4] are shown for male adult and senescent WT and KO mice. Age range: Adult: aged 15-20 weeks; Senescent: aged 27-30 months. Data are presented as mean±SEM. #p<0.01, *p<0.001.

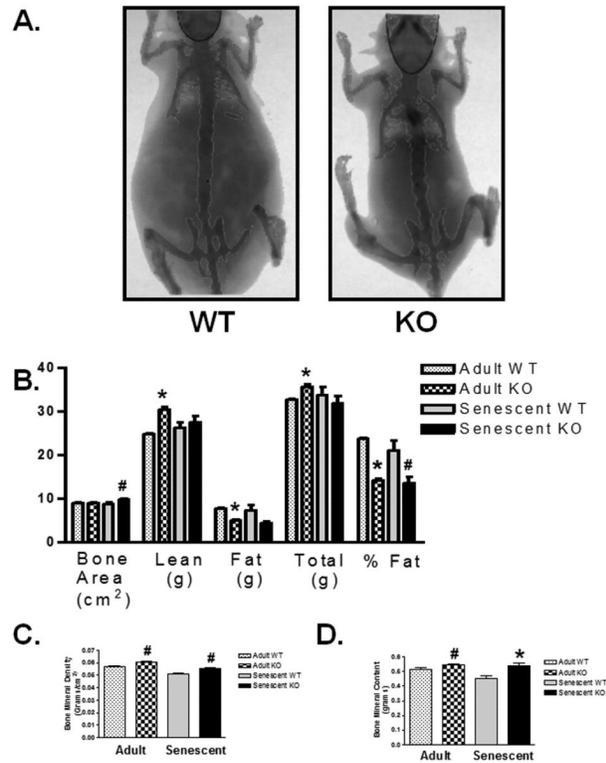


Figure 2. DEXA scan of body and bone composition in senescent mice

A) Representative DEXA scan images of senescent WT and KO mice. B) Bone area, lean mass, fat mass, total body mass, % body fat, C) bone mineral density, D) and bone mineral content as measured by DEXA scan for adult and senescent WT and KO mice. [adult WT, KO, senescent WT, KO; n=5,5,7,6 for bone measurements; n=5,5,10,8 for all other measurements]. Data are presented as mean ± SEM. #p<0.05, *p<0.01 vs age-matched WT.

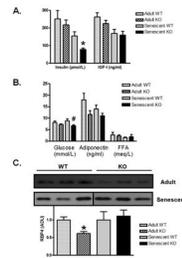


Figure 3. Decreased insulin and glucose levels in aged KO mice

Serum measurements from adult and senescent WT and KO mice are shown for A) insulin [adult WT, KO, senescent WT, KO; n=3,5,15,11], IGF-I [adult WT, KO, senescent WT, KO; n=3,5,10,6], B) glucose [adult WT, KO, senescent WT, KO; n=7,13,14,10], adiponectin [adult WT, KO, senescent WT, KO; n=3,5,15,11], free fatty acids [adult WT, KO, senescent WT, KO; n=3,5,11,6]. C) A representative western blot of RBP4 from serum (1 μ l) of adult and senescent WT and KO mice with compiled data normalized to age-matched WT [adult WT, KO, senescent WT, KO; n=3,5,11,10]. Data are presented as fold age-matched WT mean \pm SEM. #p<0.05, *p<0.01 vs age-matched WT.

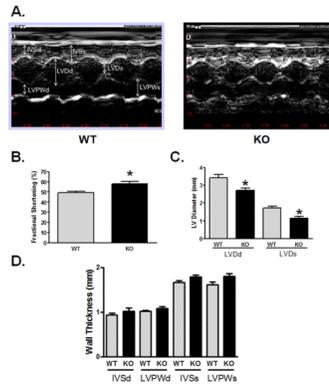


Figure 4. Echocardiographic data show preserved function and smaller LV dimensions in senescent myostatin KO mice

A) Representative m-mode images from WT (left) and KO (right) mice. Bar graphs depict cumulative echocardiographic measurements obtained in conscious male mice 27-30 months old, with heart rates between 650-750 beats per minute ($p=ns$ between WT and KO) [WT, KO; $n=8,7$]. B) Fractional shortening, C) LV Diameter, D) LV Wall thickness.

Abbreviations used: LV, left ventricle; LVDd, LV end-diastolic dimension; LVDs, LV end-systolic dimension; IVSd, intraventricular septum end-diastolic dimension; LVPWd, LV posterior wall end-diastolic dimension; IVSs, intraventricular septum end-systolic dimension; LVPWs, LV posterior wall end-systolic dimension. Data are presented as mean \pm SEM. * $p<0.01$.

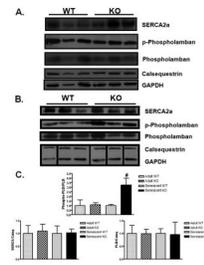


Figure 5. Increased ratio of phospho- to total phospholamban in senescent myostatin KO hearts
 A) Western blot analysis from whole heart lysates of sarcoplasmic reticulum proteins involved in calcium handling from adult and senescent WT and KO mice. B) Bar graphs represent compiled western blot data normalized to age-matched WT control. [n=3 in each group]. Data are presented as fold age-matched WT mean \pm SEM. #p<0.05 vs age-matched WT.

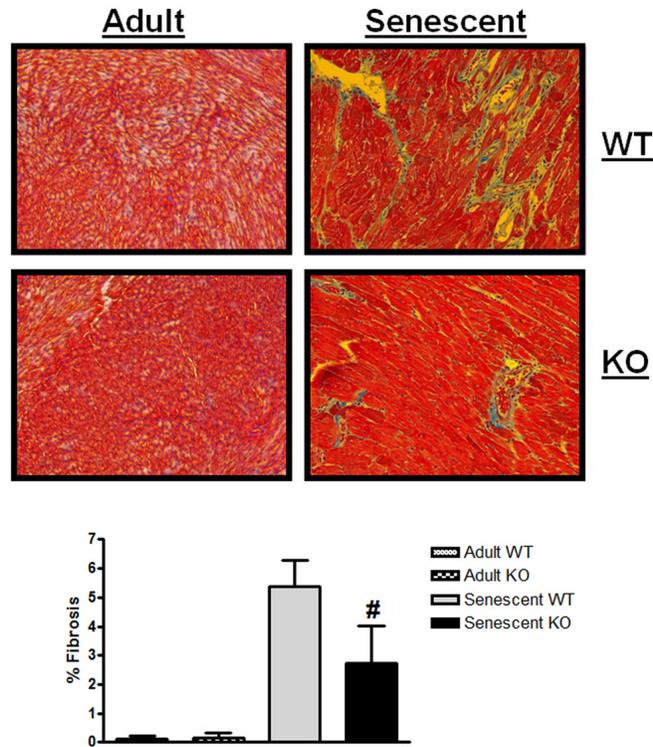


Figure 6. Senescent myostatin KO mice display less cardiac fibrosis

Representative 20X images from Masson's trichrome stained heart sections from adult and senescent WT and KO mice are displayed with percent fibrosis data compiled below [adult WT, KO, senescent WT, KO; n=3,3,4,4]. Data are presented as mean \pm SEM. #p<0.05 vs age-matched WT.